

# Strange Quark Contribution to the Vector and Axial Form Factors of the Nucleon: Combined Analysis of G0, HAPPEX, and Brookhaven E734 Data

Stephen F. Pate,<sup>\*</sup> David W. McKee<sup>†</sup>, and Vassili Papavassiliou

*Physics Department, New Mexico State University, Las Cruces NM 88003*

(Dated: October 25, 2018)

## Abstract

The strange quark contribution to the vector and axial form factors of the nucleon has been determined for momentum transfers in the range  $0.45 < Q^2 < 1.0 \text{ GeV}^2$ . The results are obtained via a combined analysis of forward-scattering, parity-violating elastic  $\vec{e}p$  asymmetry data from the G0 and HAPPEX experiments at Jefferson Lab, and elastic  $\nu p$  and  $\bar{\nu}p$  scattering data from Experiment 734 at Brookhaven National Laboratory. The parity-violating asymmetries measured in elastic  $\vec{e}p$  scattering at forward angles establish a relationship between the strange vector form factors  $G_E^s$  and  $G_M^s$ , with little sensitivity to the strange axial form factor  $G_A^s$ . On the other hand, elastic neutrino scattering at low  $Q^2$  is dominated by the axial form factor, with some significant sensitivity to the vector form factors as well. Combination of the two data sets allows the simultaneous extraction of  $G_E^s$ ,  $G_M^s$ , and  $G_A^s$  over a significant range of  $Q^2$  for the very first time. The  $Q^2$ -dependence of the strange axial form factor suggests that the strange quark contribution to the proton spin,  $\Delta s$ , is negative.

PACS numbers: 13.40.Gp, 14.20.Dh

---

<sup>†</sup> Current address: Department of Physics and Astronomy, University of Alabama, Tuscaloosa, AL, 35487

<sup>\*</sup>Electronic address: pate@nmsu.edu

## I. HISTORICAL MOTIVATION

Ever since the discovery of the first “strange” particles in cosmic ray experiments [1] and the subsequent formulation of the 3-quark model of baryons [2], nuclear and particle physicists have sought to understand the role the strange quark plays in “non-strange” particles like the proton. Data from deep-inelastic scattering of electrons and neutrinos from nucleons has determined the unpolarized momentum density  $s(x, Q^2)$  of strange quarks down to  $x \approx 10^{-4}$  [3, 4, 5]. Here,  $x$  and  $Q^2$  are respectively the Bjorken scaling variable and the positive squared four-momentum transfer for the deep-inelastic scattering vertex. These results indicate that the strange quarks account for about 5% of the nucleon momentum in the “infinite momentum frame” in which these deep-inelastic data are usually interpreted. Interest in the role of the strange quark in the nucleon deepened when the first polarized inclusive deep-inelastic measurements of the spin-dependent structure function  $g_1(x)$  by EMC [6, 7] demonstrated that the Ellis-Jaffe sum rule [8, 9] did not hold true; these data implied as well that the strange quark contribution to the proton spin,  $\Delta s$ , widely expected to be zero, was possibly negative. Subsequent measurements at CERN and SLAC supported the initial EMC measurements, and a global analysis [10] of these data suggested  $\Delta s \approx -0.15$ .

In the meantime, the E734 experiment [11] at Brookhaven measured the  $\nu p$  and  $\bar{\nu} p$  elastic scattering cross sections in the momentum-transfer range  $0.45 < Q^2 < 1.05 \text{ GeV}^2$ . These cross sections are very sensitive to the strange axial form factor of the proton,  $G_A^s(Q^2)$ , which is related to the strange quark contribution to the proton spin:  $G_A^s(Q^2 = 0) = \Delta s$  [12]. E734 also extracted a negative value for  $\Delta s$ ; however, this determination was hampered by the large systematic uncertainties in the cross section measurement, as well as a lack of knowledge of the strange vector form factors, and no definitive determination of  $\Delta s$  was possible. Subsequent reanalyses [13, 14] confirmed that the E734 data alone cannot determine  $\Delta s$ .

More recent measurements using leptonic deep-inelastic scattering have not given a clear picture of the strange quark contribution to the nucleon spin. The HERMES experiment [15] measured the helicity distribution of strange quarks,  $\Delta s(x)$ , using polarized semi-inclusive deep-inelastic scattering and a leading-order “purity” analysis, and found  $\Delta s(x) \approx 0$  in the range  $0.03 < x < 0.3$ . However, a next-to-leading-order analysis by de Florian, Navarro and Sassot [16] including these HERMES semi-inclusive data with other world-wide DIS data

found a clearly negative strange quark polarization in the same  $x$ -range. A more recent next-to-leading-order global analysis including not only leptonic deep-inelastic scattering data but also data from the collision of polarized protons at RHIC [17] suggests that  $\Delta s(x)$  may have a node at  $x \approx 0.03$ , passing from positive to negative with decreasing  $x$ . The first moment of  $\Delta s(x)$  in this fit, giving the strange quark spin contribution  $\Delta s$ , is negative.

In parallel to the effort to determine the activities of the strange quarks in the proton via deep-inelastic scattering, a strong effort has been made to measure the strange quark contribution to the elastic form factors of the proton, in particular the vector (electric and magnetic) form factors. These experiments [18, 19, 20, 21, 22, 23, 24, 25, 26, 27] exploit an interference between the  $\gamma$ -exchange and  $Z$ -exchange amplitudes in order to measure weak elastic form factors  $G_E^{Z,p}$  and  $G_M^{Z,p}$  which are the weak-interaction analogs of the more traditional electromagnetic elastic form factors  $G_E^{\gamma,p}$  and  $G_M^{\gamma,p}$  for which copious experimental data are available. The interference term is observable as a parity-violating asymmetry in elastic  $\vec{e}p$  scattering, with the electron longitudinally polarized. By combining the electromagnetic form factors of the proton and neutron with the weak form factors of the proton, one may separate the up, down, and strange quark contributions.

It is important to point out the differences between what can be measured in elastic scattering and in different kinds of deep-inelastic scattering, particularly in regards to the axial form factor. Elastic scattering of electrons or neutrinos from nucleons is a neutral current ( $\gamma$  or  $Z$ ) process that integrates over the whole proton wavefunction and so cannot easily distinguish between quark and anti-quark. The strange axial form factor,  $G_A^s$ , then is a sum over  $s$  and  $\bar{s}$  contributions, and likewise the value of  $\Delta s = G_A^s(Q^2 = 0)$  that might be extracted from those measurements is also a sum over  $s$  and  $\bar{s}$ . Similarly, inclusive leptonic deep-inelastic scattering does not distinguish between quark and anti-quark contributions. However, semi-inclusive deep-inelastic scattering, employed by the HERMES experiment using a model-dependent analysis involving fragmentation functions, can distinguish between quark and anti-quark by observing leading hardrons in the final state; observation of leading kaons gives HERMES a window into the contributions of  $s$  and  $\bar{s}$  quarks to the spin of the proton. In this manuscript, we will continue to use the notation  $\Delta s$  to refer to the sum of  $s$  and  $\bar{s}$  contributions to the spin of the proton, as might be determined from a measurement of  $G_A^s$ .

With the first HAPPEX [22] measurement of parity-violating asymmetries in elastic  $\vec{e}p$

scattering at  $Q^2 = 0.477 \text{ GeV}^2$ , it became possible to determine simultaneously [28] the strange vector and axial form factors of the proton by combining those data with the  $\nu p$  and  $\bar{\nu} p$  elastic scattering cross sections from Brookhaven E734; the result was the first determination of the strangeness contribution to the axial form factor of the proton at non-zero  $Q^2$ . Subsequently, additional parity-violating data have become available from the G0 experiment [25]. The purpose of this paper is to improve and update the analysis done in Ref. [28] by using more complete expressions for the asymmetries, by including the recent G0 data, by performing a complete uncertainty analysis, and by comparing the results with available models.

Two global analyses of the parity-violating asymmetries in elastic  $\vec{e}p$  scattering have been published recently [29, 30]. The focus of these analyses was on the vector form factors in the very low  $Q^2$  region,  $Q^2 < 0.3 \text{ GeV}^2$ , with a special interest in extrapolating to  $Q^2 = 0$  to determine the strangeness contribution to the proton magnetic moment. The emphasis here will be instead on the  $Q^2$ -dependence of these form factors, including the strange axial form factor.

## II. ELASTIC PROTON FORM FACTORS: THE STRANGENESS CONTRIBUTION

The static properties of the nucleon are described by elastic form factors defined in terms of matrix elements of current operators. For example, the matrix element for the electromagnetic current (one-photon exchange) is expressed as

$${}_N \langle p' | J_\mu^\gamma | p \rangle_N = \bar{u}(p') \left[ \gamma_\mu F_1^{\gamma,N}(Q^2) + i \frac{\sigma_{\mu\nu} q^\nu}{2M} F_2^{\gamma,N}(Q^2) \right] u(p)$$

where the matrix element is taken between nucleon states  $N$  of momenta  $p$  and  $p'$ , the momentum transfer is  $Q^2 = -(p - p')^2$ ,  $u$  is a nucleon spinor, and  $M$  is the mass of the nucleon. Similarly, the matrix element of the neutral weak current (one- $Z$  exchange) is

$$\begin{aligned} {}_N \langle p' | J_\mu^{NC} | p \rangle_N = \bar{u}(p') \left[ \gamma_\mu F_1^{Z,N}(Q^2) + i \frac{\sigma_{\mu\nu} q^\nu}{2M} F_2^{Z,N}(Q^2) \right. \\ \left. + \gamma_\mu \gamma_5 G_A^{Z,N}(Q^2) + \frac{q_\mu}{M} \gamma_5 G_P^{Z,N}(Q^2) \right] u(p). \end{aligned}$$

The form factors are respectively the Dirac and Pauli vector ( $F_1$  and  $F_2$ ), the axial ( $G_A$ ), and the pseudo-scalar ( $G_P$ ). Due to the point-like interaction between the gauge bosons

( $\gamma$  or  $Z$ ) and the quarks internal to the nucleon, these form factors can be expressed as separate contributions from each quark flavor; for example, the electromagnetic and neutral weak Dirac form factors of the proton can be expressed in terms of contributions from up, down, and strange quarks:

$$\begin{aligned} F_1^{\gamma,p} &= \frac{2}{3}F_1^u - \frac{1}{3}F_1^d - \frac{1}{3}F_1^s \\ F_1^{Z,p} &= \left(1 - \frac{8}{3}\sin^2\theta_W\right)F_1^u + \left(-1 + \frac{4}{3}\sin^2\theta_W\right)F_1^d + \left(-1 + \frac{4}{3}\sin^2\theta_W\right)F_1^s. \end{aligned}$$

The same quark form factors are involved in both expressions; the coupling constants that multiply them (electric or weak charges) correspond to the interaction involved (electromagnetic or weak neutral). These measurements are most interesting for low momentum transfers,  $Q^2 < 1.0 \text{ GeV}^2$ , as the  $Q^2 = 0$  values of these form factors represent static integral properties of the nucleon. It is common to use in these studies the Sachs electric and magnetic form factors

$$G_E = F_1 - \tau F_2 \quad G_M = F_1 + F_2 \quad (1)$$

instead of the Dirac and Pauli form factors; here,  $\tau = Q^2/4M^2$ . At  $Q^2 = 0$  the electromagnetic Sachs electric form factors take on the value of the nucleon electric charges ( $G_E^{\gamma,p}(0) = 1$ ,  $G_E^{\gamma,n}(0) = 0$ ) and the electromagnetic Sachs magnetic form factors take on the value of the nucleon magnetic moments ( $G_M^{\gamma,p}(0) = \mu_p$ ,  $G_M^{\gamma,n}(0) = \mu_n$ ). Likewise, the  $Q^2 = 0$  values of the strange quark contributions to these form factors define the strange contribution to these static quantities: for example, the strangeness contribution to the proton magnetic moment is  $\mu_s = G_M^s(Q^2 = 0)$ . It is also common in these studies to assume charge symmetry; the transformation from proton to neutron form factors is an exchange of  $u$  and  $d$  quark labels. In addition, it is generally assumed that the strange quark distributions in the proton and the neutron are the same. Then by combining the electromagnetic form factors of the proton and neutron with the weak form factors of the proton, one may separate the up, down, and strange quark contributions; for example, the electric form factors may be written as follows:

$$\begin{aligned} G_E^{\gamma,p} &= \frac{2}{3}G_E^u - \frac{1}{3}G_E^d - \frac{1}{3}G_E^s \\ G_E^{\gamma,n} &= \frac{2}{3}G_E^d - \frac{1}{3}G_E^u - \frac{1}{3}G_E^s \\ G_E^{Z,p} &= \left(1 - \frac{8}{3}\sin^2\theta_W\right)G_E^u + \left(-1 + \frac{4}{3}\sin^2\theta_W\right)G_E^d + \left(-1 + \frac{4}{3}\sin^2\theta_W\right)G_E^s. \end{aligned}$$

To attempt this separation is the motivation behind the program of parity-violating  $\vec{e}p$  scattering experiments.

The  $Z$ -exchange current involves also the axial form factor of the proton, which in a pure weak-interaction process takes this form:

$$G_A^{Z,p} = \frac{1}{2} \left( -G_A^u + G_A^d + G_A^s \right).$$

The  $u-d$  portion of this form factor is well-known from neutron  $\beta$ -decay and other charged-current ( $CC$ ) weak interaction processes like  $\nu_\mu + n \rightarrow p + \mu^-$ :

$$G_A^{CC} = G_A^u - G_A^d = \frac{g_A}{(1 + Q^2/M_A^2)^2}$$

where  $g_A = 1.2695 \pm 0.0029$  is the axial coupling constant in neutron decay [31] and  $M_A = 1.001 \pm 0.020$  is the so-called “axial mass” which is a fitting parameter for the data on this form factor [32, 33, 34]. The strange quark portion,  $G_A^s$ , is essentially unknown. In  $\nu p$  and  $\bar{\nu}p$  elastic scattering, which are pure neutral-current, weak-interaction processes, there are no significant radiative corrections to be taken into account [35], and we may safely neglect heavy quark contributions to the axial form factor [36]. On the other hand, since elastic  $ep$  scattering is not a pure weak-interaction process, then the axial form factor does not appear in a pure form; there are significant radiative corrections which carry non-trivial theoretical uncertainties. The result is that, while the measurement of parity-violating asymmetries in  $\vec{e}p$  elastic scattering is well suited to a measurement of  $G_E^s$  and  $G_M^s$ , these experiments cannot cleanly extract  $G_A^s$ . We will overcome this difficulty in this analysis by only using forward-scattering  $ep$  data, wherein the axial terms are strongly suppressed.

### III. EXPERIMENTAL MEASUREMENTS SENSITIVE TO THE STRANGENESS FORM FACTORS OF THE NUCLEON

There are two principal sources of experimental data from which the strange quark contribution to the elastic form factors of the proton may be extracted. One of these is elastic scattering of neutrinos and anti-neutrinos from protons; these data are primarily sensitive to the axial form factor. The other is the measurement of parity-violating asymmetries in elastic  $\vec{e}p$  scattering; these data are primarily sensitive to the vector form factors. This section will describe these two kinds of experiments. The following section will describe a technique to combine these two kinds of data to extract  $G_E^s$ ,  $G_M^s$ , and  $G_A^s$  simultaneously.

TABLE I: Parameters used in this analysis. Uncertainties are listed only if they were of significant size and were used to generate the uncertainties in the results. The uncertainties on the  $R$  factors are not extracted from the references, but arise from other considerations; see text for details.

Parameter	Value	Reference
$\alpha$	$7.2973 \times 10^{-3}$	[31]
$\sin^2 \theta_W$	0.23120	[31]
$G_F/(\hbar c)^3$	$1.16637 \times 10^{-5}/\text{GeV}^2$	[31]
$g_A$	$1.2695 \pm 0.0029$	[31]
$M_A$	$1.001 \pm 0.020 \text{ GeV}$	[32, 33, 34]
$3F - D$	$0.585 \pm 0.025$	[37]
$R_V^p$	$-0.045 \pm 0.045$	[31, 38]
$R_V^n$	$-0.012 \pm 0.012$	[31, 38]
$R_V^{(0)}$	$-0.012 \pm 0.012$	[31, 38]
$R_A^{T=1}$	$-0.173 \pm 0.173$	[31, 38]
$R_A^{T=0}$	$-0.253 \pm 0.253$	[31, 38]
$R_A^{(0)}$	$-0.552 \pm 0.552$	[31, 38]

### A. Parity-violating Asymmetry in Elastic $\vec{e}p$ Scattering

The interference between the neutral weak and electromagnetic currents produces a parity-violating asymmetry in  $\vec{e}p$  elastic scattering, which has been the subject of a world-wide measurement program focussed on the determination of the strange vector (electric and magnetic) form factors. For a proton target, the full expression for the parity-violating electron scattering asymmetry is [30, 38]

$$\begin{aligned}
A_{PV}^p = & -\frac{G_F Q^2}{4\sqrt{2}\pi\alpha} \frac{1}{[\epsilon(G_E^p)^2 + \tau(G_M^p)^2]} \\
& \times \{(\epsilon(G_E^p)^2 + \tau(G_M^p)^2)(1 - 4\sin^2 \theta_W)(1 + R_V^p) \\
& - (\epsilon G_E^p G_E^n + \tau G_M^p G_M^n)(1 + R_V^n) \\
& - (\epsilon G_E^p G_E^s + \tau G_M^p G_M^s)(1 + R_V^{(0)}) \\
& - \epsilon'(1 - 4\sin^2 \theta_W)G_M^p G_A^e\}, \tag{2}
\end{aligned}$$

where the kinematics factors are

$$\begin{aligned}\epsilon &= \left[1 + 2(1 + \tau) \tan^2(\theta_e/2)\right]^{-1} \\ \epsilon' &= \sqrt{(1 - \epsilon^2)\tau(1 + \tau)}.\end{aligned}$$

The axial form factor seen in electron scattering,  $G_A^e$ , as mentioned earlier, does not appear in its pure form, but is complicated by radiative corrections:

$$G_A^e(Q^2) = G_A^{CC}(Q^2)(1 + R_A^{T=1}) + \sqrt{3}G_A^s(Q^2)R_A^{T=0} + G_A^s(Q^2)(1 + R_A^{(0)}). \quad (3)$$

The  $R$  factors appearing in Equations 2 and 3 are radiative corrections that may be expressed [38] in terms of standard model parameters [31]. Because these radiative corrections are calculated at  $Q^2 = 0$  and have an unknown  $Q^2$ -dependence, then in our analysis some additional uncertainty needs to be attributed to these radiative correction factors; we have assigned a 100% uncertainty to take the unknown  $Q^2$ -dependence into account (see Table I). Recently, a reevaluation of these radiative corrections and their uncertainties, in the context of a fit to world data on parity-violating  $\vec{e}p$  scattering, was discussed in Ref. [30]. Those values differ from the ones we have used here; however, the use of these slightly different values would not have significantly changed the results of the work presented here because of the suppression of the axial terms in the parity-violating asymmetries at forward angles.

For the vector form factors  $G_E^p$ ,  $G_E^n$ ,  $G_M^p$ , and  $G_M^n$  we have used the values given by the parametrization of Kelly [39]. The uncertainties in the vector form factors do not contribute significantly to the uncertainties in the results reported here. For the charged-current (isovector) axial form factor,  $G_A^{CC}$ , as already mentioned, we use a dipole form factor shape where the  $Q^2 = 0$  value is  $g_A = 1.2695 \pm 0.0029$  [31] and the  $Q^2$ -dependence is given by the “axial mass” parameter  $M_A = 1.001 \pm 0.020$  [32, 33, 34]. The selection of a correct parametrization of  $G_A^{CC}$  is crucial to the correct extraction of  $G_A^s$  from neutrino neutral-current data because those data are sensitive to the total neutral-current axial form factor  $G_A^{Z,p} = (-G_A^{CC} + G_A^s)/2$ . Any shift in the value of  $G_A^{CC}$  will produce a shift in the extracted value of  $G_A^s$ . We chose to use the  $M_A$  from Refs. [32, 33, 34] because they used up-to-date data on the vector form factors and the value of  $g_A$  and performed a thorough re-evaluation of the original deuterium data on which the value of  $M_A$  is traditionally based. Recently, two modern neutrino experiments using nuclear targets (oxygen [40] and carbon [41]) have reported higher effective values of  $M_A$  from an analysis of charge-current, quasi-elastic scattering. It not clear at this time what impact these new results have for the value of  $M_A$  for



the proton. If a significantly new set of values for  $G_A^{CC}$  for the proton can be established, then the results for  $G_A^s$  presented in this article will need to be re-evaluated. In this context it is interesting to note that Kuzmin, Lyubushkin, and Naumov [42] have analyzed a broad range of neutrino charged-current reaction data, on a wide variety of nuclear targets, and determined a value for  $M_A$  in agreement with Refs. [32, 33, 34]; this supports our use of the value  $M_A = 1.001 \pm 0.020$ .

Appearing in Equation 3 for  $G_A^e$  is the octet axial form factor  $G_A^s(Q^2)$ . The  $Q^2 = 0$  value of this form factor is the quantity  $(3F - D)/2\sqrt{3}$ ; we have taken the value of  $3F - D$  from a recent fit in Ref. [37] (see Table I). We took the  $Q^2$ -dependence of  $G_A^s$  to be the same as that of  $G_A^{CC}$ , i.e.

$$G_A^s(Q^2) = \frac{(3F - D)/2\sqrt{3}}{(1 + Q^2/M_A^2)^2}$$

but this is an assumption. This form factor is multiplied by the radiative correction factor  $R_A^{T=0}$  to which we have already assigned a 100% uncertainty because we did not know its  $Q^2$ -dependence; as a result, we assigned no additional uncertainty to  $G_A^s$ .

The parity-violating asymmetry may be written as a linear combination of the strange electric form factor ( $G_E^s$ ), the strange magnetic form factor ( $G_M^s$ ), and the strange axial form factor ( $G_A^s$ ), as follows:

$$A_{PV}^p = A_0^p + A_E^p G_E^s + A_M^p G_M^s + A_A^p G_A^s$$

where the coefficients are

$$\begin{aligned} A_0^p &= -K^p \left\{ \begin{aligned} &\epsilon G_E^p \left[ (1 - 4\sin^2 \theta_W)(1 + R_V^p)G_E^p - (1 + R_V^n)G_E^n \right] \\ &+ \tau G_M^p \left[ (1 - 4\sin^2 \theta_W)(1 + R_V^p)G_M^p - (1 + R_V^n)G_M^n \right] \\ &- \epsilon' G_M^p (1 - 4\sin^2 \theta_W) \left[ (1 + R_A^{T=1})G_A^{CC} + \sqrt{3}R_A^{T=0}G_A^s \right] \end{aligned} \right\} \\ A_E^p &= K^p \left\{ \epsilon G_E^p (1 + R_V^0) \right\} \\ A_M^p &= K^p \left\{ \tau G_M^p (1 + R_V^0) \right\} \\ A_A^p &= K^p \left\{ \epsilon' G_M^p (1 - 4\sin^2 \theta_W)(1 + R_A^0) \right\} \\ K^p &= \frac{G_F Q^2}{4\pi\sqrt{2}\alpha} \frac{1}{\epsilon G_E^{p\,2} + \tau G_M^{p\,2}}. \end{aligned}$$

It is well to note that the axial term in this asymmetry is suppressed by the weak electron charge ( $1 - 4\sin^2 \theta_W \approx 0.075$ ), and at forward angles it is suppressed additionally by the kinematic factor  $\epsilon'$ . This might seem a disadvantage, since this strongly suppresses the

sensitivity to the strange axial form factor in  $G_A^e$ ; however, it simultaneously suppresses the uncertainty in the radiative corrections in  $G_A^e$  which are significant in magnitude and have an unknown  $Q^2$ -dependence. Therefore, the parity-violating asymmetry data serve to provide a necessary constraint among the strange vector form factors, with only a little sensitivity to the strange axial form factor.

## B. Cross Section for Elastic $\nu p$ and $\bar{\nu} p$ Scattering

The neutral weak interaction ( $Z$ -exchange) process is uniquely sensitive to the strange axial form factor. The cross section for  $\nu p$  and  $\bar{\nu} p$  elastic scattering is given by

$$\frac{d\sigma}{dQ^2} = \frac{G_F^2}{2\pi} \frac{Q^2}{E_\nu^2} (A \pm BW + CW^2) \quad (4)$$

where the  $+$  ( $-$ ) sign is for  $\nu$  ( $\bar{\nu}$ ) scattering, and

$$\begin{aligned} W &= 4(E_\nu/M_p - \tau) \\ \tau &= Q^2/4M_p^2 \\ A &= \frac{1}{4} \left[ (G_A^Z)^2 (1 + \tau) - ((F_1^Z)^2 - \tau(F_2^Z)^2) (1 - \tau) + 4\tau F_1^Z F_2^Z \right] \\ B &= -\frac{1}{4} G_A^Z (F_1^Z + F_2^Z) \\ C &= \frac{1}{64\tau} \left[ (G_A^Z)^2 + (F_1^Z)^2 + \tau(F_2^Z)^2 \right]. \end{aligned}$$

The dependence on the strange form factors is contained in the neutral current form factors  $F_1^Z$ ,  $F_2^Z$ , and  $G_A^Z$ . At low  $Q^2$ , this cross section is dominated by the axial form factor,

$$\frac{d\sigma}{dQ^2} \stackrel{\nu p \rightarrow \nu p}{(Q^2 \rightarrow 0)} = \frac{G_F^2}{32\pi} \frac{M_p^2}{E_\nu^2} \left[ (G_A^Z)^2 + (1 - 4\sin^2 \theta_W)^2 \right], \quad (5)$$

so these data are a primary source of information about the strange axial form factor. Data on these cross sections exists in the range  $0.45 < Q^2 < 1.05 \text{ GeV}^2$  from the Brookhaven E734 experiment — see Table II. Due to a variety of experimental and analytical difficulties, these data have large total uncertainties, typically 20-25%.

## IV. COMBINED ANALYSIS OF BNL E734, HAPPEX, AND G0 DATA

A technique for combining forward-scattering parity-violating  $\vec{e}p$  asymmetry data with elastic  $\nu p$  and  $\bar{\nu} p$  data was previously used to combine the data from HAPPEX [22, 43]

TABLE II: Differential cross section data from BNL E734 [11]. The uncertainties shown are total; they include statistical,  $Q^2$ -dependent systematic, and  $Q^2$ -independent systematic contributions, all added in quadrature. Also listed is the correlation coefficient  $\rho$  for the  $\nu$  and  $\bar{\nu}$  data at each value of  $Q^2$ .

$Q^2$ GeV <sup>2</sup>	$d\sigma/dQ^2(\nu p)$ 10 <sup>-12</sup> (fm/GeV) <sup>2</sup>	$d\sigma/dQ^2(\bar{\nu} p)$ 10 <sup>-12</sup> (fm/GeV) <sup>2</sup>	Correlation Coefficient
0.45	0.165 ± 0.033	0.0756 ± 0.0164	0.13
0.55	0.109 ± 0.017	0.0426 ± 0.0062	0.26
0.65	0.0803 ± 0.0120	0.0283 ± 0.0037	0.29
0.75	0.0657 ± 0.0098	0.0184 ± 0.0027	0.26
0.85	0.0447 ± 0.0090	0.0129 ± 0.0023	0.16
0.95	0.0294 ± 0.0073	0.0108 ± 0.0022	0.12
1.05	0.0205 ± 0.0063	0.0101 ± 0.0027	0.07

and Brookhaven Experiment E734 [11] to extract  $G_E^s$ ,  $G_M^s$ ,  $G_A^s$  at  $Q^2 = 0.5$  GeV<sup>2</sup> [28]. In the present article we extend that analysis to include also the recent forward-scattering G0 data [25] to extract these form factors in the range  $0.45 < Q^2 < 1.0$  GeV<sup>2</sup>. (Table III lists the parity-violating asymmetries used in the analysis described here.) Some small improvements were made in the numerical procedures in the meantime — especially, the full expression for the parity-violating asymmetry  $A_{PV}$  is now used, instead of just the linear combination of  $G_E^s$  and  $G_M^s$  reported by the experiments as was done in Ref. [28]. A number of the parameters needed for this more complete analysis have already been discussed; a list of the parameters is given in Table I.

The data from E734 and that from HAPPEX and G0 are not reported at the same  $Q^2$  values. The values of  $Q^2$  in HAPPEX and G0 are rather precisely determined, while the results from E734 are averaged over bins in  $Q^2$  that are 0.1 GeV<sup>2</sup> wide. As a result we interpolated the E734 data (cross-sections, uncertainties, and correlation coefficients) to the  $Q^2$  values of the data from HAPPEX and G0. Because the E734 results already contain a systematic uncertainty due to the  $Q^2$ -determination [11], we did not attribute any additional uncertainty to our interpolation.

Because the neutrino-proton elastic scattering cross sections (Equation 4) contain

TABLE III: Parity-violating asymmetries from the HAPPEX[22, 43] and G0[25] experiments that have been used in this analysis.

Experiment	$Q^2$	$A_{PV}$
	GeV <sup>2</sup>	ppm
HAPPEX	0.477	$-14.92 \pm 1.13$
G0	0.511	$-16.81 \pm 2.29$
G0	0.631	$-19.96 \pm 2.14$
G0	0.788	$-30.8 \pm 4.13$
G0	0.997	$-37.9 \pm 11.54$

quadratic combinations of the strange form factors, there will be two solutions when these data are combined with the parity-violating asymmetries (which are linear in the strange form factors, Equation 2). The quadratic nature of the neutrino data also make difficult an algebraic method of solution, and so a numerical procedure was developed.

In Table IV the results of the combining of these data at each value of  $Q^2$  are shown. As mentioned, there are two solutions at each  $Q^2$ . Other available data must be used to determine which one is the physical solution. The two solutions have distinct features, and there are three strong reasons to prefer Solution 1:

- (1) The values of  $G_E^s$  in Solution 2 are always positive, large in magnitude ( $\approx 0.3$ ) and several standard deviations away from zero. However, we do not expect  $G_E^s$  to be large; we expect it to be small, perhaps zero, since the net electric charge from strangeness in the nucleon is zero. This expectation has been borne out in the results of the HAPPEX measurements at  $Q^2 = 0.1$  GeV<sup>2</sup> [27] which report  $G_E^s = -0.005 \pm 0.019$ . In Solution 1,  $G_E^s$  is indeed consistent with zero.
- (2) The values of  $G_M^s$  in Solution 2 are always negative, moderate to large in magnitude ( $\approx -0.2$  to  $-0.9$ ), and several standard deviations away from zero. All of the indications from experiment so far concerning  $G_M^s$  are that it may be small and positive, or perhaps zero [20, 27]; Solution 1 is consistent with these existing indications.
- (3) The values of  $G_A^s$  in Solution 2 are always positive, moderate in magnitude ( $\approx 0.2$ ), and several standard deviations away from zero. The estimates we have from DIS

experiments are that  $\Delta s = G_A^s(Q^2 = 0)$  is either zero or small and negative [15, 16, 17]; Solution 1 is consistent with those estimates.

For these reasons, we select Solution 1 as the physical solution.

TABLE IV: Strange form factors for  $0.45 < Q^2 < 1.0 \text{ GeV}^2$  produced from the E734 and G0 data. Both Solutions 1 and 2 are shown. Solution 2 is ruled out by other experimental data, as explained in the text.

$Q^2$ (GeV <sup>2</sup> )	Solution 1			Solution 2		
	$G_E^s$	$G_M^s$	$G_A^s$	$G_E^s$	$G_M^s$	$G_A^s$
0.477	$0.02 \pm 0.12$	$0.00 \pm 0.29$	$-0.127 \pm 0.062$	$0.39 \pm 0.06$	$-0.94 \pm 0.15$	$0.266 \pm 0.127$
0.511	$0.01 \pm 0.10$	$0.03 \pm 0.22$	$-0.103 \pm 0.051$	$0.37 \pm 0.05$	$-0.81 \pm 0.12$	$0.257 \pm 0.102$
0.631	$0.02 \pm 0.07$	$0.08 \pm 0.11$	$-0.046 \pm 0.032$	$0.31 \pm 0.03$	$-0.47 \pm 0.06$	$0.221 \pm 0.060$
0.788	$-0.02 \pm 0.07$	$0.08 \pm 0.08$	$-0.021 \pm 0.029$	$0.25 \pm 0.03$	$-0.31 \pm 0.05$	$0.180 \pm 0.050$
0.997	$-0.13 \pm 0.10$	$0.22 \pm 0.07$	$0.015 \pm 0.040$	$0.23 \pm 0.06$	$-0.17 \pm 0.06$	$0.225 \pm 0.045$

## A. Discussion of the Results

Figure 1 displays the results (Solution 1) as a function of  $Q^2$ , along with some model calculations that we discuss in Section V. Also shown in this figure are the results of the global analysis by Liu et al. [30] of low- $Q^2$  parity-violating electron scattering (PVES) data; that analysis gives a result for the strange vector form factors  $G_E^s$  and  $G_M^s$  at  $Q^2=0.1 \text{ GeV}^2$  but not for  $G_A^s$  for the reasons discussed earlier. (Ref. [29] has also determined  $G_E^s$  and  $G_M^s$  at  $Q^2 = 0.1 \text{ GeV}^2$  using the same data as in Ref. [30]; the results are consistent with those of Ref. [30] but the uncertainties are very much larger.) The analysis given here, combining a single PVES asymmetry (G0 or HAPPEX) with the  $\nu p$  and  $\bar{\nu} p$  data, determines  $G_M^s$  with a similar precision as is found from the global fit of multiple PVES asymmetries. On the other hand, the PVES data do a spectacular job in determining  $G_E^s$ . The real benefit of the analysis given here, of course, is the determination of the strangeness contribution to the axial form factor,  $G_A^s$ , which shows a trend towards negative values with decreasing  $Q^2$ . This would suggest that  $\Delta s = G_A^s(Q^2 = 0)$  may be negative as well, but it is clear from

Figure 1 that the available data do not extend to sufficiently low  $Q^2$  and are not yet precise enough to make a definitive statement.

## B. Correlations among the Results

It is important to discuss the point-to-point correlations that exist in these results. We present these in two different areas: correlations between different  $Q^2$  points for a given form factor, and correlations between different form factors at a given value of  $Q^2$ .

**Correlations for results for a given form factor:** These correlations arise out of the interpolation of the E734 data points to the  $Q^2$  values of the PV (HAPPEX and G0) data points. The interpolation results in a “sharing” of E734 points between various PV data points, and so the results obtained at the PV  $Q^2$  points are not independent of each other. We express this correlation in terms of a correlation coefficient,  $\rho_{ab} = \frac{\sigma_{ab}^2}{\sigma_a \sigma_b}$ , where  $\sigma_{ab}^2$  is the covariance between results  $a$  and  $b$ , and  $\sigma_a$  and  $\sigma_b$  are the standard deviations for results  $a$  and  $b$ . The only non-zero correlations of this type are between the 0.477 and 0.511 GeV<sup>2</sup> points, the 0.477 and 0.631 GeV<sup>2</sup> points, and the 0.511 and 0.631 GeV<sup>2</sup> points; these are displayed in Table V.

TABLE V: Non-zero correlation coefficients for different  $Q^2$  points for a given form factor. The notation  $\rho(Q_1^2, Q_2^2)$  refers to a correlation between the values of the given form factor at  $Q_1^2$  and  $Q_2^2$ .

Form Factor	$\rho(0.477, 0.511)$	$\rho(0.477, 0.631)$	$\rho(0.511, 0.631)$
$G_E^s$	0.891	0.046	0.193
$G_M^s$	0.905	0.055	0.191
$G_A^s$	0.884	0.038	0.189

**Correlations for results for a given  $Q^2$ :** These correlations simply express the lack of linear independence of the results, which is itself due to the algebraic expressions that must be numerically solved to extract the three strange form factors. These are displayed as correlation coefficients in Table VI; these correlations are not very strong.

TABLE VI: Correlation coefficients among the form factors at a given value of  $Q^2$ .

$Q^2$ GeV <sup>2</sup>	$\rho(G_E^s, G_M^s)$	$\rho(G_E^s, G_A^s)$	$\rho(G_M^s, G_A^s)$
0.477	-0.199	0.060	-0.061
0.511	-0.187	0.034	-0.034
0.631	-0.187	-0.017	0.024
0.788	-0.169	-0.049	0.064
0.997	-0.118	-0.122	0.115

## V. COMPARISON TO MODEL CALCULATIONS

It is interesting to compare these results with models that can calculate a  $Q^2$ -dependence for these form factors. We distinguish between those models that provide a calculation of all three form factors (electric, magnetic and axial — see Fig. 1) and those that only provide a calculation of the vector form factors (electric and magnetic — see Fig. 2).

Silva, Kim, Urbano and Goeke [46, 47, 48] have used the chiral quark soliton model ( $\chi$ QSM) to calculate  $G_{E,M,A}^s(Q^2)$  in the range  $0.0 < Q^2 < 1.0$  GeV<sup>2</sup>. The  $\chi$ QSM has been very successful in reproducing other properties of light baryons using only a few parameters which are fixed by other data. In Figure 1 their calculation is shown as the long-dashed line. Riska, An, and Zou [49, 50, 51] have explored the strangeness content of the proton by writing all possible  $uuds\bar{s}$  configurations and considering their contributions to  $G_{E,M,A}^s(Q^2)$ . They find that a unique  $uuds\bar{s}$  configuration, with the  $s$  quark in a  $P$  state and the  $\bar{s}$  in an  $S$  state, gives the best fit to the data for these form factors; see the short-dashed lines in Figure 1. Lyubovitskij, Wang, Gutsche, and Faessler [45] have studied these form factors in the framework of the perturbative chiral quark model; see the thin solid line in Figure 1. Finally, Park and Weigel [44] have employed the SU(3) Skyrme model including vector mesons; see the thick solid line in Figure 1.

It is remarkable that none of these models give a satisfactory description for all three form factors. Refs. [45] and [49, 50, 51] give a good description of the vector form factors, especially the tight constraint placed by the Liu et al. fit on  $G_E^s$  at  $Q^2 = 0.1$  GeV<sup>2</sup>, but fall short of describing  $G_A^s$  well. On the other hand, Ref. [46, 47, 48] does the best job on  $G_A^s$

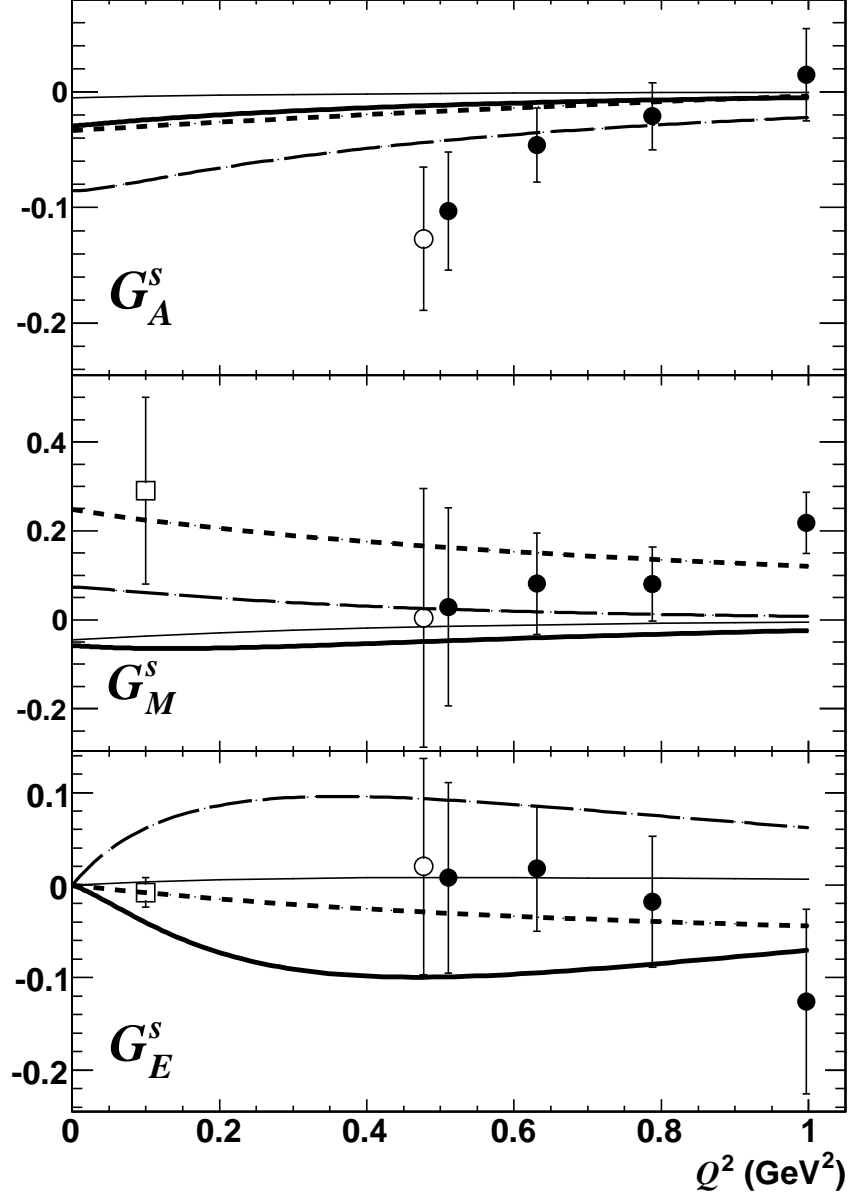


FIG. 1: Results of this analysis for the strange vector and axial form factors of the proton. Open circles are from a combination of HAPPEX and E734 data, while the closed circles are from a combination of G0 and E734 data. [Open squares at  $Q^2 = 0.1 \text{ GeV}^2$  are from Ref. [30] and involve parity-violating elastic electron scattering data only.] The theoretical curves are from models that calculate all three of these form factors: Park and Weigel [44] (thick solid line); Lyubovitskij, Wang, Gutsche, and Faessler [45] (thin solid line); Silva, Kim, Urbano and Goeke [46, 47, 48] (long-dashed line); and Riska, An, and Zou [49, 50, 51] (short-dashed line).



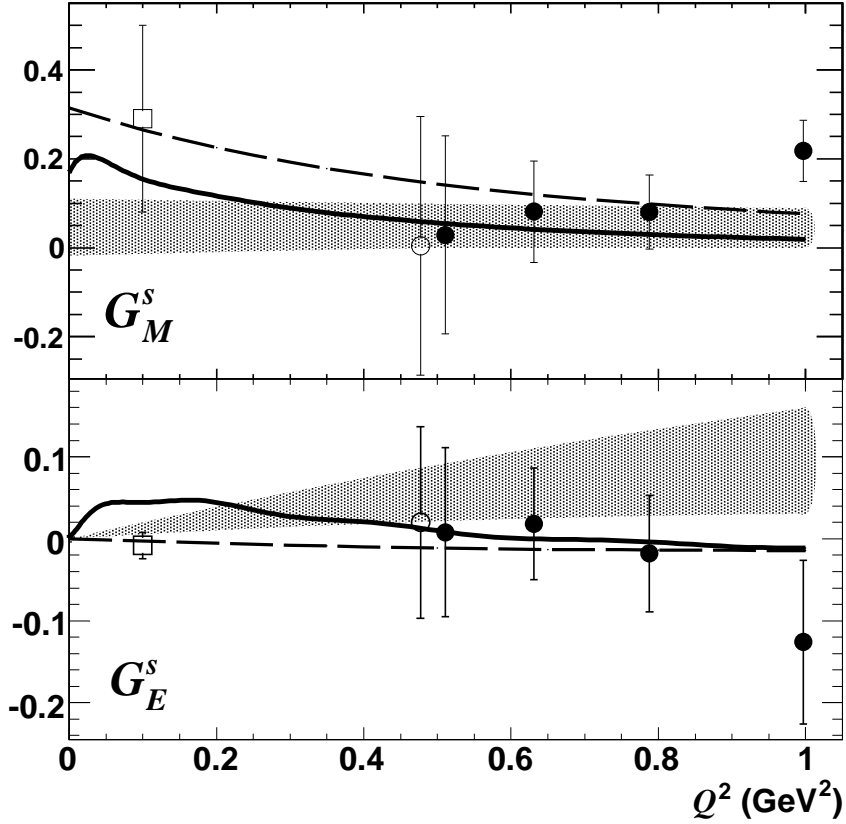


FIG. 2: Same data as in Figure 1 for the strange vector form factors of the proton, shown in comparison to models which only calculate these two form factors: Weigel, Abada, Alkofer and Reinhardt [52] (thick solid line); Bijker [53] (long-dashed line); and Lewis, Wilcox, and Woloshyn [54] (the shaded bands show the upper and lower limits of these quantities from this model).

but gives a large value for  $G_E^s$  at  $Q^2 = 0.1 \text{ GeV}^2$ .

Next we consider theoretical models which only provided calculations of the vector form factors. Weigel, Abada, Alkofer and Reinhardt [52] have calculated the strange vector form factors of the nucleon in the Nambu-Jona-Lasinio soliton model using the collective approach

of Yabu and Ando; their calculation is the thick solid line in Figure 2. Bijker [53] uses a two-component model of the nucleon in which the external photon couples to both an intrinsic internal structure and to a meson cloud through the intermediate vector mesons ( $\rho$ ,  $\omega$ ,  $\phi$ ); the strange quark content comes from the meson cloud component. His results are shown as the long-dashed line in Figure 2. Finally, Lewis, Wilcox, and Woloshyn [54] have combined quenched lattice QCD calculations with quenched chiral perturbation theory to calculate the strangeness contribution to the vector form factors; the shaded bands in Figure 2 show the limits on these quantities from their model. Two of these models, Refs. [53] and [54], provide a satisfactory description of the vector form factors — it would be interesting to see what these models have to say about the axial form factor as well.

It is worth noting that Cherman and Cohen [55] have recently questioned the validity of the calculation of the strangeness content of the nucleon from chiral soliton models similar to those used in Refs. [46, 47, 48] and [52].

## VI. FUTURE EXPERIMENTS

The analysis presented here provides evidence that  $G_A^s(Q^2)$  becomes negative with decreasing  $Q^2$ , implying that  $\Delta s = G_A^s(Q^2 = 0)$  may itself be negative. In the near future, the PVA4 experiment [56] will present final backward-angle PVES data at 0.23 GeV<sup>2</sup>, and also the G0 experiment will provide backward-angle PVES data at 0.23 and 0.63 GeV<sup>2</sup>. These new data should greatly constrain the strange vector form factors at these  $Q^2$  points, and will additionally constrain  $G_A^s$  to some extent; the backward-angle data are more sensitive to the axial form factor than are the forward-angle data. However, additional (and more precise)  $\nu p$  and  $\bar{\nu} p$  elastic scattering data, extended to lower  $Q^2$  values, are needed for a definite determination of the axial and also the vector form factors.

Several existing and proposed experiments may provide improved neutrino data in both the near and far term. The MiniBooNE experiment [57] has already a preliminary result for  $\nu p$  elastic scattering cross sections that could additionally constrain the strange axial form factor  $G_A^s$ . The SciBooNE experiment [58], which has completed a run already at Fermilab, may be able to provide  $\nu p$  elastic scattering cross sections as well. FINESS [59] proposes to measure the ratio of the neutral-current to the charged-current  $\nu N$  and  $\bar{\nu} N$  processes. A measurement of  $R_{NC/CC} = \sigma(\nu p \rightarrow \nu p)/\sigma(\nu n \rightarrow \mu^- p)$  and  $\bar{R}_{NC/CC} = \sigma(\bar{\nu} p \rightarrow \bar{\nu} p)/\sigma(\bar{\nu} p \rightarrow$

$\mu^+n$ ) combined with the world's data on forward-scattering PV  $ep$  data can produce a dense set of data points for  $G_A^s$  in the range  $0.25 < Q^2 < 0.75 \text{ GeV}^2$  with an uncertainty at each point of about  $\pm 0.02$ . Another experiment with similar physics goals, called NeuSpin [60], is being proposed for the new JPARC facility in Japan.

It is also important to extend the semi-inclusive deep-inelastic data to smaller  $x$  and higher  $Q^2$  so that the determination of the polarized strange quark distribution  $\Delta s(x)$  can be improved. The COMPASS experiment [61] will extend the HERMES measurement of  $\Delta s(x)$  in just this way, and a measurement of this type is also envisioned [62, 63] for the proposed electron-ion collider facility. It is only with these improved data sets that we will be able to arrive at an understanding of the strange quark contribution to the proton spin.

The authors are grateful to S.D. Bass, H.E. Jackson, D.O. Riska, A.W. Thomas, J. Arvieux, E. Beise, E. Leader, R. Young, and T.W. Donnelly for useful discussions. This work was supported by the US Department of Energy, Office of Science.

- 
- [1] G. D. Rochester and C. C. Butler, *Nature* **160**, 855 (1947).
  - [2] M. Gell-Mann, *Phys. Lett.* **8**, 214 (1964).
  - [3] J. Pumplin et al., *JHEP* **07**, 012 (2002).
  - [4] A. D. Martin, R. G. Roberts, W. J. Stirling, and R. S. Thorne, *Eur. Phys. J.* **C23**, 73 (2002).
  - [5] H. L. Lai et al., *JHEP* **04**, 089 (2007).
  - [6] J. Ashman et al. (European Muon Collaboration), *Phys. Lett.* **B206**, 364 (1988).
  - [7] J. Ashman et al. (European Muon Collaboration), *Nucl. Phys.* **B328**, 1 (1989).
  - [8] J. R. Ellis and R. L. Jaffe, *Phys. Rev.* **D9**, 1444 (1974).
  - [9] J. Ellis and R. Jaffe, *Phys. Rev. D* **10**, 1669 (1974).
  - [10] B. W. Filippone and X.-D. Ji, *Advances in Nuclear Physics* **26**, 1 (2001).
  - [11] L. A. Ahrens et al., *Phys. Rev.* **D35**, 785 (1987).
  - [12] M. Anselmino, A. Efremov, and E. Leader, *Phys. Rept.* **261**, 1 (1995).
  - [13] G. T. Garvey, W. C. Louis, and D. H. White, *Phys. Rev.* **C48**, 761 (1993).
  - [14] W. M. Alberico et al., *Nucl. Phys.* **A651**, 277 (1999).
  - [15] A. Airapetian et al. (HERMES), *Phys. Rev.* **D71**, 012003 (2005).
  - [16] D. de Florian, G. A. Navarro, and R. Sassot, *Phys. Rev.* **D71**, 094018 (2005).

- [17] D. de Florian, R. Sassot, M. Stratmann, and W. Vogelsang (2008), arXiv:0804.0422.
- [18] B. Mueller et al. (SAMPLE), Phys. Rev. Lett. **78**, 3824 (1997).
- [19] R. Hasty et al. (SAMPLE), Science **290**, 2117 (2000).
- [20] D. T. Spayde et al. (SAMPLE), Phys. Lett. **B583**, 79 (2004).
- [21] T. M. Ito (SAMPLE), Phys. Rev. Lett. **92**, 102003 (2004).
- [22] K. A. Aniol et al. (HAPPEX), Phys. Rev. **C69**, 065501 (2004).
- [23] F. E. Maas et al. (A4), Phys. Rev. Lett. **93**, 022002 (2004).
- [24] F. E. Maas et al., Phys. Rev. Lett. **94**, 152001 (2005).
- [25] D. S. Armstrong et al. (G0), Phys. Rev. Lett. **95**, 092001 (2005).
- [26] K. A. Aniol et al. (HAPPEX), Phys. Lett. **B635**, 275 (2006).
- [27] A. Acha et al. (HAPPEX), Phys. Rev. Lett. **98**, 032301 (2007).
- [28] S. F. Pate, Phys. Rev. Lett. **92**, 082002 (2004).
- [29] R. D. Young, J. Roche, R. D. Carlini, and A. W. Thomas, Phys. Rev. Lett. **97**, 102002 (2006).
- [30] J. Liu, R. D. McKeown, and M. J. Ramsey-Musolf, Phys. Rev. **C76**, 025202 (2007).
- [31] S. Eidelman et al. (Particle Data Group), Phys. Lett. **B592**, 1 (2004).
- [32] A. Bodek, H. Budd, and J. Arrington, AIP Conf. Proc. **698**, 148 (2004).
- [33] H. Budd, A. Bodek, and J. Arrington (2003), hep-ex/0308005.
- [34] H. Budd, A. Bodek, and J. Arrington, Nucl. Phys. Proc. Suppl. **139**, 90 (2005).
- [35] W. J. Marciano and A. Sirlin, Phys. Rev. **D22**, 2695 (1980).
- [36] S. D. Bass, R. J. Crewther, F. M. Steffens, and A. W. Thomas, Phys. Rev. **D66**, 031901 (2002).
- [37] Y. Goto et al. (Asymmetry Analysis), Phys. Rev. **D62**, 034017 (2000).
- [38] M. J. Musolf et al., Phys. Rept. **239**, 1 (1994).
- [39] J. J. Kelly, Phys. Rev. **C70**, 068202 (2004).
- [40] R. Gran et al. (K2K), Phys. Rev. **D74**, 052002 (2006).
- [41] A. A. Aguilar-Arevalo et al. (MiniBooNE), Phys. Rev. Lett. **100**, 032301 (2008).
- [42] K. S. Kuzmin, V. V. Lyubushkin, and V. A. Naumov, Eur. Phys. J. **C54**, 517 (2008).
- [43] K. A. Aniol et al. (HAPPEX), Phys. Lett. **B509**, 211 (2001).
- [44] N. W. Park and H. Weigel, Nucl. Phys. **A541**, 453 (1992).
- [45] V. E. Lyubovitskij, P. Wang, T. Gutsche, and A. Faessler, Phys. Rev. **C66**, 055204 (2002).
- [46] A. Silva, H.-C. Kim, D. Urbano, and K. Goeke, Phys. Rev. **D72**, 094011 (2005).

- [47] K. Goeke, H.-C. Kim, A. Silva, and D. Urbano, Eur. Phys. J. **A32**, 393 (2007).
- [48] A. Silva, H.-C. Kim, D. Urbano, and K. Goeke, Phys. Rev. **D74**, 054011 (2006).
- [49] B. S. Zou and D. O. Riska, Phys. Rev. Lett. **95**, 072001 (2005).
- [50] C. S. An, D. O. Riska, and B. S. Zou, Phys. Rev. **C73**, 035207 (2006).
- [51] D. O. Riska and B. S. Zou, Phys. Lett. **B636**, 265 (2006).
- [52] H. Weigel, A. Abada, R. Alkofer, and H. Reinhardt, Phys. Lett. **B353**, 20 (1995).
- [53] R. Bijker, J. Phys. **G32**, L49 (2006).
- [54] R. Lewis, W. Wilcox, and R. M. Woloshyn, Phys. Rev. **D67**, 013003 (2003).
- [55] A. Cherman and T. D. Cohen, Phys. Lett. **B651**, 39 (2007).
- [56] S. Baunack, Eur. Phys. J. **A32**, 457 (2007).
- [57] D. C. Cox (MiniBooNE), AIP Conf. Proc. **967**, 130 (2007).
- [58] J. L. Alcaraz-Aunion and J. Catala-Perez, AIP Conf. Proc. **967**, 307 (2007).
- [59] L. Bugel et al. (FINeSSE) (2004), hep-ex/0402007.
- [60] Y. Miyachi, T.-A. Shibata, and N. Saito, AIP Conf. Proc. **915**, 387 (2007).
- [61] CERN Report CERN-SPSC-2007-002 (2007).
- [62] U. Stösslein and E. R. Kinney, AIP Conf. Proc. **588**, 171 (2001).
- [63] A. Deshpande, R. Milner, R. Venugopalan, and W. Vogelsang, Ann. Rev. Nucl. Part. Sci. **55**, 165 (2005).